ENVIRONMENTAL RESEARCH
LETTERS

LETTER • OPEN ACCESS

Exploring risks and benefits of overshooting a 1.5 °C carbon budget over space and time

To cite this article: Nico Bauer *et al* 2023 *Environ. Res. Lett.* **18** 054015

ENVIRONMENTAL RESEARCH
LETTERS

CrossMark

OPEN ACCESS

RECEIVED
3 November 2022

REVISED
29 March 2023

ACCEPTED FOR PUBLICATION
17 April 2023

PUBLISHED
2 May 2023

LETTER

Exploring risks and benefits of overshooting a 1.5 °C carbon budget over space and time

Nico Bauer[1,*], David P Keller[2], Julius Garbe[1,3], Kristine Karstens[1], Franziska Piontek[1], Werner von Bloh[1], Wim Thiery[4], Maria Zeitz[1,3], Matthias Mengel[1], Jessica Strefler[1], Kirsten Thonicke[1] and Ricarda Winkelmann[1,3]

[1] Potsdam Institute for Climate Impact Research (PIK), Member of the Leibniz Association, Potsdam, Germany
[2] GEOMAR Helmholtz Centre for Ocean Research, Kiel, Germany
[3] Institute of Physics and Astronomy, University of Potsdam, Potsdam, Germany
[4] Vrije Universiteit Brussel, Department of Hydrology and Hydraulic Engineering, Brussels, Belgium
[*] Author to whom any correspondence should be addressed.

E-mail: nico.bauer@pik-potsdam.de

Keywords: carbon dioxide removal, mitigation and impacts, integrated assessment models, Earth system model of intermediate complexity, global south, carbon budget overshoot

Supplementary material for this article is available online

Abstract

Temperature targets of the Paris Agreement limit global net cumulative emissions to very tight carbon budgets. The possibility to overshoot the budget and offset near-term excess emissions by net-negative emissions is considered economically attractive as it eases near-term mitigation pressure. While potential side effects of carbon removal deployment are discussed extensively, the additional climate risks and the impacts and damages have attracted less attention. We link six models for an integrative analysis of the climatic, environmental and socio-economic consequences of temporarily overshooting a carbon budget consistent with the 1.5 °C temperature target along the cause-effect chain from emissions and carbon removals to climate risks and impact. Global climatic indicators such as CO_2-concentration and mean temperature closely follow the carbon budget overshoot with mid-century peaks of 50 ppmv and 0.35 °C, respectively. Our findings highlight that investigating overshoot scenarios requires temporally and spatially differentiated analysis of climate, environmental and socioeconomic systems. We find persistent and spatially heterogeneous differences in the distribution of carbon across various pools, ocean heat content, sea-level rise as well as economic damages. Moreover, we find that key impacts, including degradation of marine ecosystem, heat wave exposure and economic damages, are more severe in equatorial areas than in higher latitudes, although absolute temperature changes being stronger in higher latitudes. The detrimental effects of a 1.5 °C warming and the additional effects due to overshoots are strongest in non-OECD countries (Organization for Economic Cooperation and Development). Constraining the overshoot inflates CO_2 prices, thus shifting carbon removal towards early afforestation while reducing the total cumulative deployment only slightly, while mitigation costs increase sharply in developing countries. Thus, scenarios with carbon budget overshoots can reverse global mean temperature increase but imply more persistent and geographically heterogeneous impacts. Overall, the decision about overshooting implies more severe trade-offs between mitigation and impacts in developing countries.

1. Introduction

The temperature targets of the Paris Agreement can be translated into carbon budgets (e.g. Meinshausen *et al* 2009) as the global mean temperature (GMT) shows a short-term albeit permanent response to cumulative emissions (e.g. Matthews *et al* 2009). Only for very large overshoot magnitudes and durations the symmetric temperature response to net positive and net-negative emission fluxes vanishes (e.g. Jones *et al* 2016, Zickfeld *et al* 2016). The focus on GMT inhibits quantification of temporal and spatial responses of systems and processes along the cause-effect chain from (i) emissions and removals through (ii) the climate system to (iii) impacts and damages. In this study we explore the differences between two scenarios that differ only in the overshoot of the carbon budget.

Integrated assessment models (IAMs) derived overshoot magnitudes of up to 1000 $GtCO_2$ above the carbon budget until 2100 (Bauer *et al* 2018, Riahi *et al* 2021). The main argument in support of overshooting is the lower near-term mitigation costs. The positive economic effect is stronger the smaller the carbon budget (Kriegler *et al* 2014, Bauer *et al* 2018, Riahi *et al* 2021). Riahi *et al* (2021) identified potential positive effects on annual GDP of limiting the overshoot during the 2nd half of the 21st century. The overshoot magnitude also depends on the development of the climate policy ambition over time that can be measured by the carbon price path (Realmonte *et al* 2019, Strefler *et al* 2021a). Stronger near-term policy ambition results in deeper near-term emission reductions and larger deployment of carbon dioxide removal technologies (Riahi *et al* 2021, Strefler *et al* 2021a). This can aggravate environmental problems related to carbon removals such as bioenergy with carbon capture and storage (BECCS; Smith *et al* 2015, Heck *et al* 2018). A broader portfolio of carbon removal options tends to increase overshoots, but reduces overspecialization on a single option with spatially concentrated harmful effects (Strefler *et al* 2021b).

Climate models are used to assess resulting additional climate risks. The overshoots are simulated by assuming: (i) single year removal pulses of 370 to nearly 2000 $GtCO_2$, (ii) emission-driven scenarios lead to different cumulative CO_2-emissions or (iii) concentration driven runs differ by several thousand $GtCO_2$ of cumulative emissions. Asymmetric and non-linear GMT changes to single year pulses of CO_2-emissions or removals have been demonstrated if they are large or imposed on different equilibrium states (Zickfeld *et al* 2021). Variations of CO_2-concentration overshoot scenarios identified additional climate risks due to inertia and path-dependency regarding carbon pools, ocean heat and sea-level rise (SLR) (Boucher *et al* 2012, MacDougall 2013, Tokarska and Zickfeld 2015, Zickfeld *et al* 2016, Palter *et al* 2017). These studies are difficult to interpret because concentration driven scenarios feature GMT differences up to 1.5 °C (Boucher *et al* 2012). Later studies extended the analysis to oceanic biogeochemistry (e.g. Mathesius *et al* 2015, Hofmann *et al* 2019).

The additional socioeconomic risks are under-researched. A recent study by Drouet *et al* (2021) investigated overshoot scenarios with maximum GMT difference of 0.16 °C, based on the MAGICC model. Differences of indicators representing heat and drought were 'statistically indistinguishable' and showed no regional patterns. Also additional SLR would not exceed 2.3 cm by 2200. Different to that, the overshoot causes no less than 4 trillion USD/yr of GDP reduction by 2100 , if the damage function relied on Burke *et al* (2015).

Based on the existing literature it is difficult to assess overshoots because studies are mostly narrowly focused, use incoherent scenario assumptions and vary in their temporal and spatial focus. The present study addresses these shortcomings. First, we use a broad set of models to assess effects of carbon budget overshoot along the whole cause–effect chain considering, climatic and environmental issues. Second, we will not only consider emissions and removals, but also land-use change information derived with an IAM to drive Earth system models and models mof relevant components. Third, we will investigate the temporal and geographical impacts of mitigation benefits and induced additional climate risks to better understand reversibility and trade-off relationships.

2. Integrated framework of models

For the evaluation of the overshoot flexibility, we integrate a series of models from different disciplines into an analysis framework (figure 1). The models are peer-reviewed and used by international assessment bodies, such as the Intergovernmental Panel on Climate Change (IPCC).

The framework works through the cause-effect chain, but information does not feedback between models to fully close the loop. For example, climate impacts and damages are based on socioeconomic factors and policies, but these socioeconomic developments and policies that drive the emissions in REMIND-MAgPIE. Similarly, the climatic effects on terrestrial vegetation computed with LPJmL are not fed back into the UVic model to update the carbon cycle representation and, thus, improve information about carbon fluxes. The socio-economic assumptions are harmonized to the middle-of-the-road scenario of the Shared Socioeconomic Pathways (SSPs, Kriegler *et al* 2017).

The REMIND-MAgPIE model computes the emission and land-use pathways with full and minimal overshoot flexibility. It derives scenarios for CO_2 emissions and other climate forcers as well as land-use patterns consistent with deployment patterns of CDR technologies: BECCS, afforestation, direct air capture and storage (DACS) and enhanced weathering (Strefler *et al* 2021b). The 1.5 °C target at 66% no-exceedance likelihood is implemented by a global carbon budget with 600 $GtCO_2$ for the time horizon 2010–2100 (Rogelj *et al* 2018, 2019). Emissions and removals are controlled by a globally uniform carbon price that starts in 2025 and grows at 5% per year. All other GHG emissions are priced using CO_2-eq

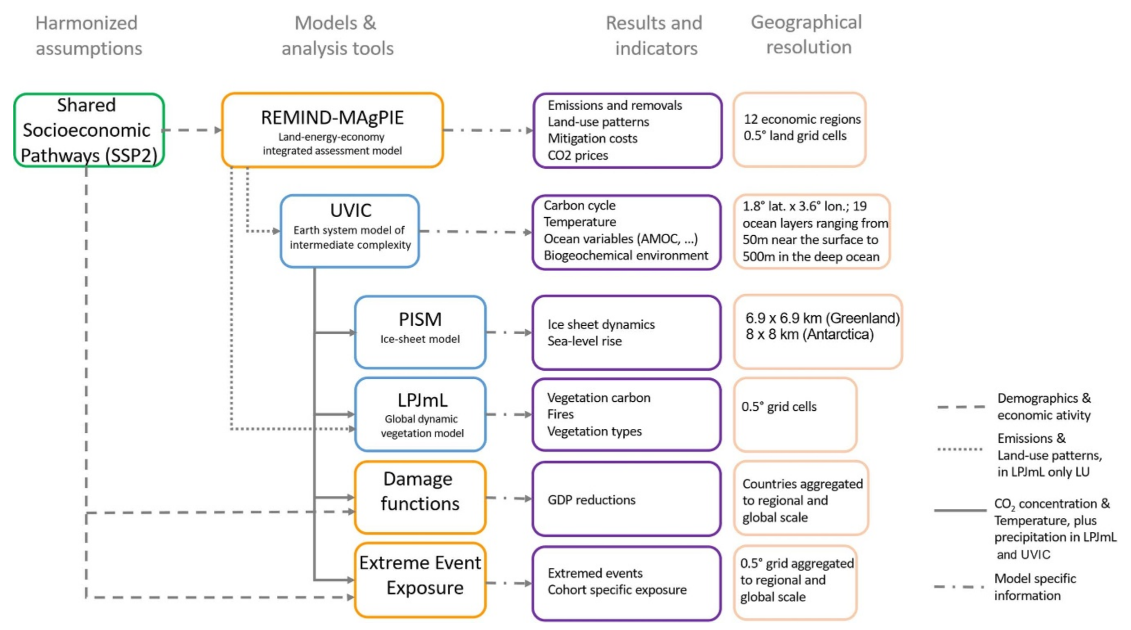

Figure 1. Overview on information flow of the integrated model framework. REMIND-MAgPIE: Bauer *et al* (2020b), Strefler *et al* (2021b); UVic 2.10—Mengis *et al* (2020); PISM—Winkelmann *et al* (2011), Bueler and Brown (2009); LPJmL—Schaphoff *et al* (2018); Macroeconomic damages—Burke *et al* (2015), Schultes *et al* (2021); Life-time extreme event exposure—Thiery *et al* (2021).

conversion factors based on Global Warming Potentials (GWP100). Aerosol emissions such as sulfur and black carbon are also represented depending on human activities. In the scenarios of this study the resulting overall radiative forcing of aerosols decreases because the relevant activity levels decline and the emission factor decrease due to assumed air pollution policies (Rao *et al* 2017).

The carbon budget is small and cannot be achieved in the model by completely avoiding a budget overshoot. Hence, we limit the over-shoot and name it minimal or low overshoot scenario. In this scenario net-negative emissions are not remunerated. In the full overshoot scenario all net-negative emissions are remunerated at the level of the carbon price. Thus, the duration and magnitude of the overshoot is derived endogenously given the socioeconomic conditions and the strength of the climate target. We also perform a sensitivity analysis that gradually reduces the overshoot by varying the remuneration factor.

The emission and land-use scenarios are used by the UVic model (Mengis *et al* 2020) to simulate climatic and biogeochemical changes. The model provides insights into the dynamic changes of natural carbon pools (including the permafrost soils), atmospheric temperatures, precipitation, sea-ice, oceanic heat content and thermosteric expansion, ocean circulation as well as marine and terrestrial biogeochemistry. The model adequately simulates changes in historical temperature and carbon fluxes for the historical period 1850–2015 (Mengis *et al* 2020). The model is also used to investigate parametric uncertainties (see SI).

The UVic model serves as the basis to evaluate a broad spectrum of changes in the climate system at the global level and is spatially resolved. For a more comprehensive assessment and integrated perspective we use the results of UVic and REMIND-MAgPIE to force a broader portfolio of models allowing us to evaluate impacts on more climate, environmental and socioeconomic systems (figure 1).

The temperature and precipitation changes of UVic are used by the Parallel Ice Sheet Model (PISM, Bueler and Brown 2009, Winkelmann *et al* 2011, Garbe *et al* 2020) to evaluate the impacts on the ice sheets of Greenland and Antarctica and resulting contributions to SLR that is added to the ocean thermal expansion and glacier melting. PISM simulates mass changes due to snowing, melting and ice discharge (Calov and Greve 2005, Reese *et al* 2018, Zeitz *et al* 2021). Additionally, the temperature changes as well as the ice sheet geometry changes caused by the melting lead to an increase in dynamic ice losses, further contributing to SLR. The contribution of glaciers to SLR is evaluated using a parsimonious emulator approach by Mengel *et al* (2016) that parameterizes the results of 18 different climate models and separates the effect of anthropogenic warming from natural factors. The resulting sensitivity curves for SLR driven by glacier melting show the largest long-term equilibrium SLR for long-term global warming of up to 2 °C. The SLR contribution from thermosteric expansion due to ocean heating is taken from the UVic runs.

The global terrestrial vegetation model LPJmL uses the global CO_2-concentration, temperature, precipitation, radiation and land-use patterns from REMIND-MAgPIE and UVic (figure 1). All climate variables are used from the years 1901–1930 and randomly shuffled. It allows to evaluate the impacts on the vegetation and changes in the spatial distribution of biomes and potential degradation. Compared to UVic's terrestrial carbon cycle model LPJmL uses a finer spatial and temporal resolution, comprises more detailed processes, a broader set of vegetation types and an advanced representation of fire dynamics. We use LPJmL to detect hotspots of changes in terrestrial carbon pools and relate it to climatic or land-use changes.

Changes in economic activity are related to GMT changes (Burke *et al* 2015). The relation is hump-shaped with a maximum at ~13 °C. A change in one-year GMT shock implies change in the level of GDP with uncertain degree of permanence (Newell *et al* 2020, Piontek *et al* 2018). Thus, we formulate a decay function and vary the half-time in years after which half of the original annual GDP effect is still present (Schultes *et al* 2021). In this study we assume permanence of five and 15 years along with the extreme values of zero and infinity for single year damage and fully permanent GDP reduction. The damages are calculated at country-level, using population-weighted mean country temperature anomalies based on the UVic simulations and GDP per capita (Dellink *et al* 2017, KC and Lutz 2017).

Finally, we quantify the impacts on the exposure to extreme weather events over the lifetime of different age cohorts born between 1960 and 2020 (Thiery *et al* 2021). The gridded population scenarios are mapped to the spatially explicit simulations of six extreme event categories (Lange *et al* 2020): heatwaves, tropical cyclones, river floods, crop failures, wildfires and droughts. The results are summarized aggregating the frequency of extreme events over the remaining life-times per cohort. The cumulation over life-time provides a first indicator on potentially negative socioeconomic impacts, incl. more permanent consequences such as lower human capital formation due to reduced schooling.

3. Results

3.1. Overshoot, emissions, land-use change, carbon removals and costs

Net emissions would need to decrease immediately and quickly to minimize the carbon budget overshoot (figure 2(a)). In the overshoot scenario global CO_2 emissions remain constant until 2030, which exceeds the range of 1.5 °C-compatible scenarios considered by the sixth Assessment Report of the IPCC (AR6). The overshoot reaches 700GtCO_2 (see figure 2(b)), while cumulative carbon removal are 900GtCO_2 with large contributions of BECCS and DACS. The full overshoot leads net-zero CO_2 emissions in 2065 and 27 GtCO_2/yr net negative emissions by 2100, which is 5 times the mass flow of today's oil extraction. In case with only minimum overshoot in 2030 net CO_2 emissions are reduced by 70% compared with 2020, which is comparable to the fastest reduction scenarios considered in AR6.

Limiting the overshoot (moving left-to-right along the *x*-axis in figure 2(b)) lowers carbon removals only slightly as removals are increasingly used to offset intratemporally rather than intertemporally (see also Johansson *et al* 2020, Strefler *et al* 2021a). Further, afforestation on pasture and range lands becomes more important (see figure 2(c)) particularly in non-Organization for Economic Cooperation and Development (OECD) regions (figure S1(e)) offering the near-term potential to achieve net zero carbon emissions as soon as 2040 (see figure 2(a)).

Carbon prices vary substantially (in 2030 50–500US$/t$CO_2$) depending on the overshoot (figure 2(e)). The reduction in GDP is substantially higher in non-OECD countries and also varies more strongly than in OECD countries (figure 2(d)). The time profile indicates that limiting the overshoot leads to larger macroeconomic impact in non-OECD countries. During the second half of the 21st century the annual GDP reductions are lower without overshoot, but this difference is relatively small (see figure S2). This asymmetric and regressive impact is due to differences in socioeconomic development and fossil fuel dependency (Bauer *et al* 2020a).

3.2. Climate system and carbon cycle

The global CO_2 concentration in 2100 is slightly lower in the overshoot scenario (figure 3(a)), whereas the GMT is narrowed to only 20% of the peak difference (figure 4(a)). Thus, for these scenarios key global climate variables show temporary rather than persistent effects.

In the full overshoot scenario terrestrial carbon reservoirs respond within a decade turning from sink to source after atmospheric CO_2 peaked (figure 3(b)). Additional permafrost carbon losses (20GtCO_2) due to temperature feedbacks are irreversible (figure 3(d)), but they are offset by a greening vegetation. However, the carbon loss from permafrost soils may be more responsive to the overshoot due thermokarst dynamics from rapid warming (McGuire *et al* 2018, Pihl *et al* 2021). Overall, responses of the terrestrial carbon stocks are highly uncertain (Friedlingstein *et al* 2014, Hewitt *et al* 2016, Melnikova *et al* 2021, Pihl *et al* 2021). Specifically, in the overshoot the CO_2 fertilization effect weakens, while heterotroph respiration of previously accumulated carbon becomes dominant turning the vegetation system into a net-CO_2 source. The relative

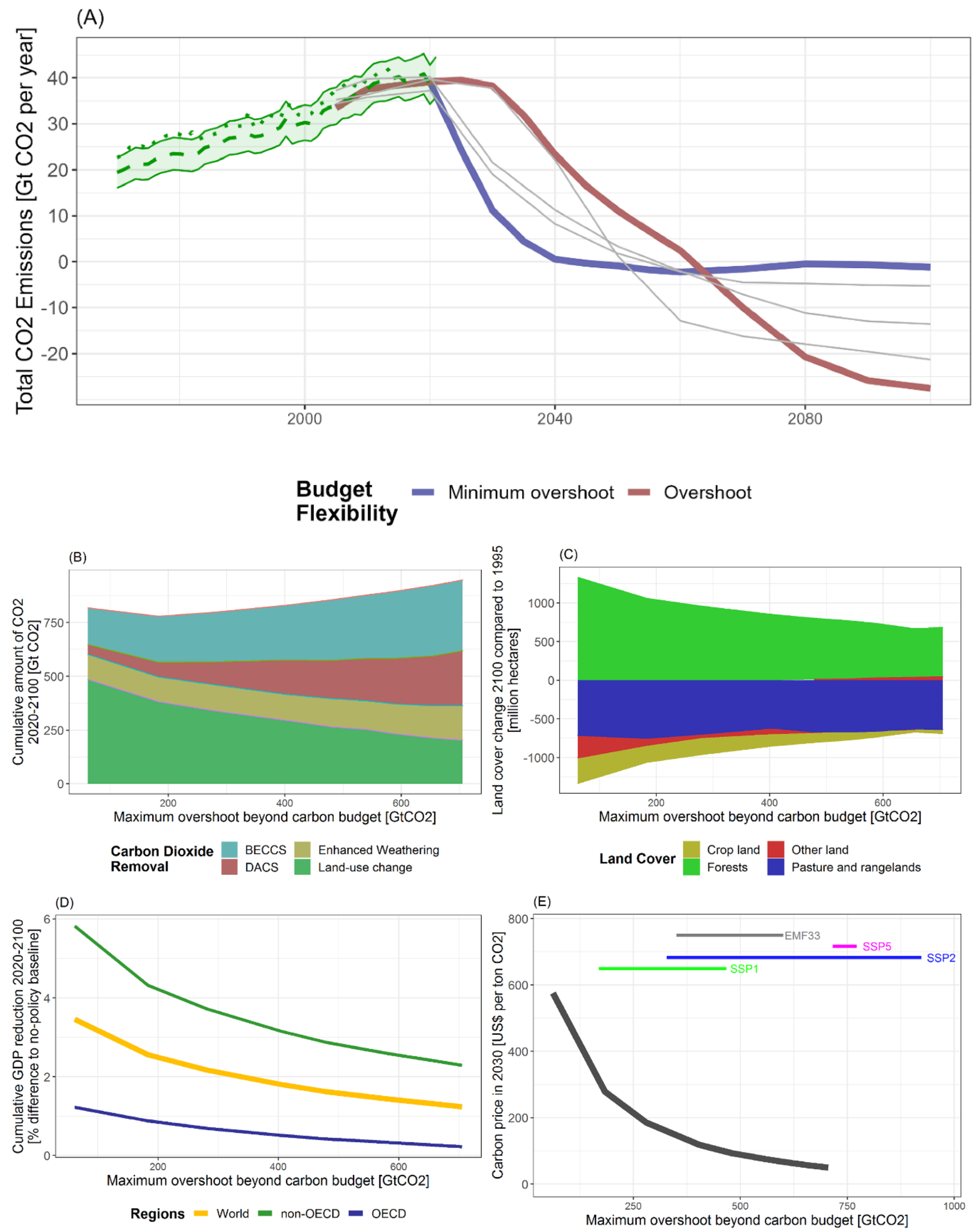

Figure 2. Overshoot flexibility and implications derived with REMIND-MAgPIE. Panel (A) shows global total net CO_2 emissions along with three illustrative scenarios of the IPCC SR15 (grey lines); the green dashed line shows the total CO_2 emissions and the uncertainty range according to the Global Carbon Project (Friedlingstein *et al* 2022) the dotted line shows historical emissions according to CEDS; see supplement for details. Note that the minimum overshoot scenario requires cumulative net negative emissions of 50 $GtCO_2$ to comply with the 600 $GtCO_2$ carbon budget. Panel (B) depicts the cumulative global carbon removals until 2100 against the global carbon budget overshoot on the *x*-axis. Panel (C) shows changes in land-cover until 2100 that are used in the UVic model. Panel (D) shows the cumulative global GDP reduction and in OECD and non-OECD countries. The numbers represent relative differences of net present values for the time horizon 2020–2100 assuming a discount rate of 5% per year. Panel (E) shows the carbon price in 2030 against the carbon budget overshoot and added the cross-model ranges of cumulative amounts of net-negative carbon emissions for three SSPs in case of the 1.9 W m^{-2} target.

magnitude of both effects is uncertain. The ocean also takes up more carbon in the overshoot scenario (figure S3(a)) and turns from sink to source only in 2080 (figure 3(c)). On balance the high CO_2 concentration leads to more carbon uptake by the vegetation and the oceans than the temperature feedback releases carbon from permafrost soils. The results are robust against variations of uncertain model parameters.

Climate systems show more persistent effects between both scenarios although GMT nearly fully

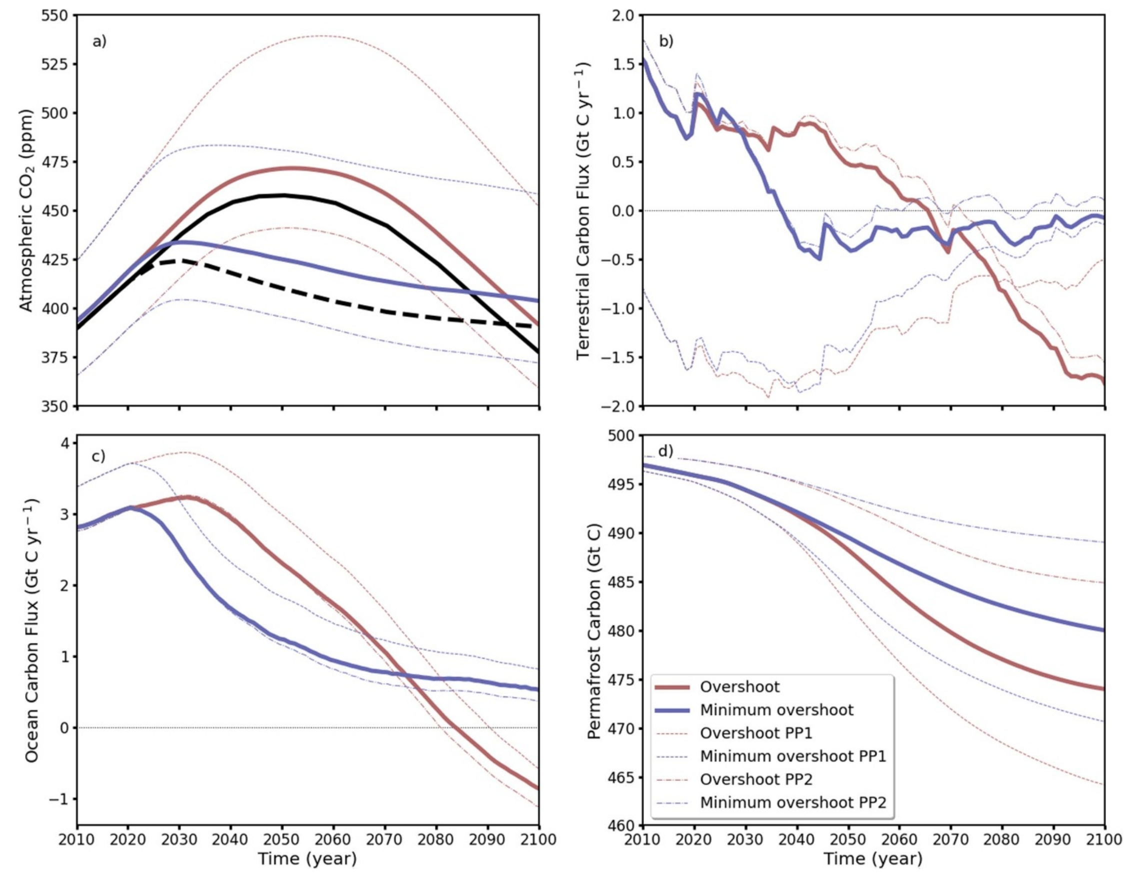

Figure 3. Comparison of UVic simulated global annual mean changes in (a) atmospheric CO_2, (b) terrestrial carbon fluxes (positive into the land), (c) the air-sea carbon flux (positive into the ocean), and (d) permafrost carbon. The black lines in (a) are the results from the MAGICC model. The dotted and dash-dotted lines are from perturbed parameter simulations that were chosen to investigate potential upper (dotted; PP1) and lower (dash-dotted; PP2) temperature responses to the forcing in these scenarios. Note: atmospheric CO_2 in both UVic scenarios (figure 3(a)) is slightly higher than in MAGICC, a behavioral bias that often occurs when ESMs are forced with emissions (Hoffman *et al* 2014). However, the biases are nearly equal in both scenarios (i.e. differences of the UVic and the MAGICC results are of a similar magnitude for both scenarios).

converges by 2100 (figure 4). The peak temperature difference between the scenarios occurs around 2065 reaching 0.35° C, upper end of the scenarios recently considered in AR6. This difference vanishes by 80% until 2100. The remaining 20% are related to higher emissions of non-CO_2 forcing agents in the overshoot scenario (see figure S8). Although GMT is nearly fully reversible by 2100 various climate systems, particularly oceans, show more persistent effects (figures 4(b)–(f)).

The ocean heat content differs between scenarios (figure 4(b)). While global annual mean sea surface temperature anomalies mostly follow atmospheric temperature change trends, deep ocean warming occurs more slowly and is driven by both mixing and diffusion as well as large-scale circulation (Gleckler *et al* 2006, Gregory *et al* 2013, figure S6). Most of the additional ocean heat storage in the overshoot scenario until 2100 occurs in the upper ocean (above 2000 m). However, warmer waters can be seen moving on circulatory pathways into the ocean interior, i.e. on the North Atlantic Deep Water, Antarctic Intermediate Water, and Antarctic Bottom Water pathways (figure S6(c)). Consequently, deeper ocean layers (below the mixed layer depth, but mostly still in the upper 2000 m) show persistent temperature differences.

Warming in both scenarios is largest at high latitudes due to polar amplification (up to 3.8 and 4.5° C above pre-industrial conditions at peak warming in the minimum overshoot and overshoot scenarios, respectively; not shown). The largest temperature differences reach 0.8 °C for near surface air temperature and ocean temperatures (figures S4 and S5(a)). Moreover, the differences vanish less than the GMT towards the poles (>0.1 °C remain by 2100, figure S5(b)). The latitudinal bias of the temperature signal and the persistence of the heat retention have various knock-on effects.

The increasing temperatures lead to ocean sea-ice melting, weakening of meridional overturning, and more precipitation (figures 4(c)–(e)). The additional peak loss is about half a million additional square kilometers. Sea-ice begins to recover from the overshoot, but at a slower rate than near-surface air temperature and 40% of the peak difference remains in 2100. Furthermore, additional precipitation doubles and is persistent throughout the century; the global

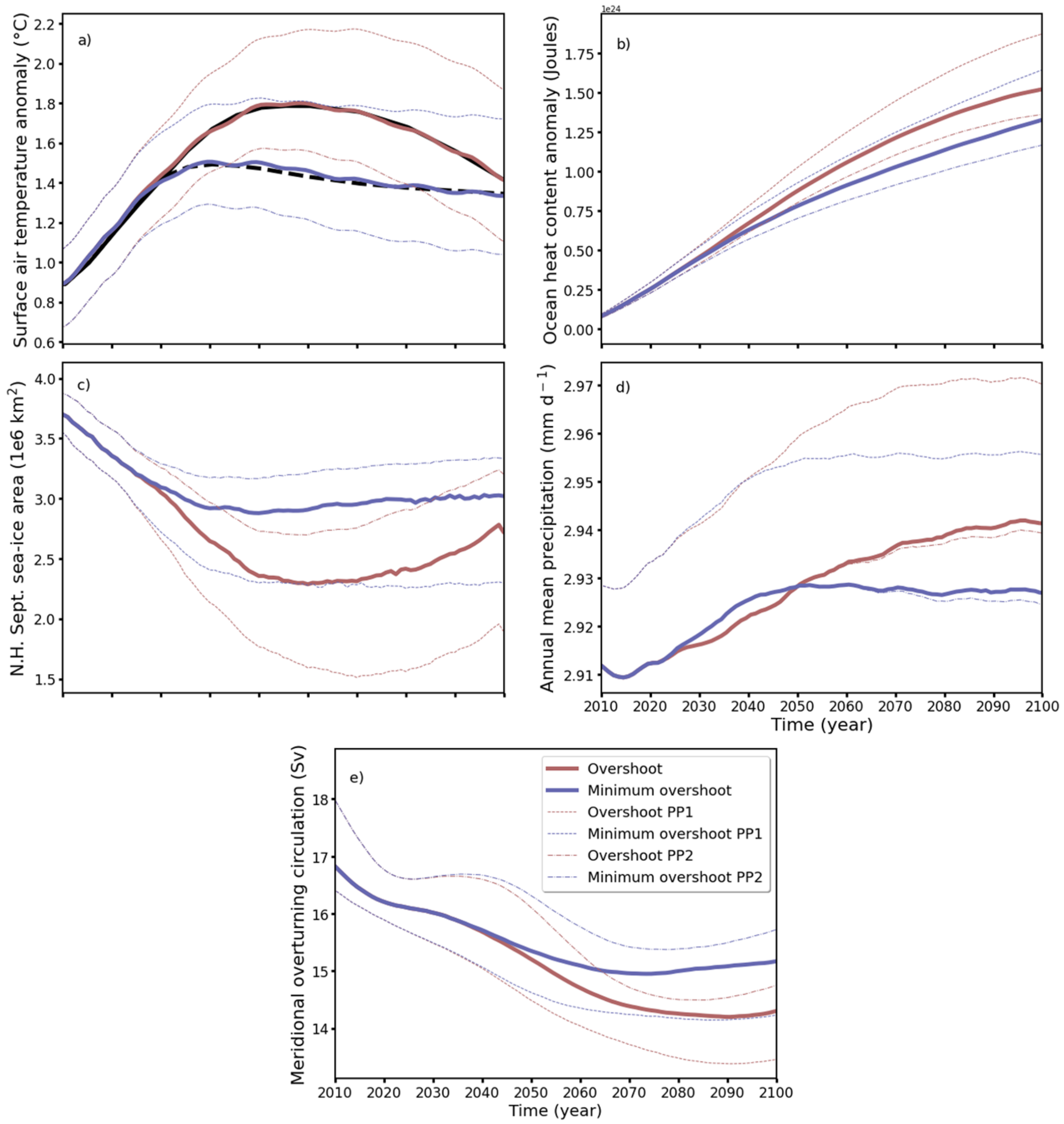

Figure 4. Comparison of UVic simulated global annual mean changes or anomalies in (a) near surface air temperature, (b) ocean heat content from 0 to 2000 m, (c) Northern hemisphere sea ice area, (d) precipitation, and (e) meridional overturning circulation. The black lines in (a) are the results from the MAGICC model. The dotted and dash-dotted lines are from perturbed parameter simulations that were chosen to investigate potential upper (dotted; PP1) and lower (dash-dotted; PP2) temperature responses to the forcing in these scenarios.

anomaly is maximum 2% and mostly related to oceans. Also, the weakening of the meridional overturning is twice as strong in case with the overshoot, but this effect is more persistent and shows hardly any recovery until 2100 (figure 4(e)). Finally, warmer oceans contribute to stronger SLR, which is treated next.

3.3. Ice sheets and sea-level rise

The scenario with minimal overshoot leads to long-lasting SLR driven by ice dynamics for both the Antarctica and Greenland ice-sheets as well as mountain glaciers and thermosteric expansion from warming oceans (figure 5). In the minimal-overshoot scenario the SLRs continuously by 39.7 cm until 2100, which is comparable with the best-estimate 41 cm assessed in AR6 WG1 for the 1.5 °C scenario. The temperature overshoot leads to an additional SLR of 3.6 cm or nearly 10% until 2100 that continues growing thereafter (figures 5(b), (d), (f), (h)). The additional SLR exceeds the estimates of 0.4–2.3 cm until 2200 by Drouet *et al* (2021) substantially.

The major SLR driver until 2100 is thermosteric expansion with 19.4 cm in the low-overshoot scenario adding another 2.8 cm at time of the peak difference in 2080. In both scenarios the ocean heat content increases until and beyond 2100 (figure 4(b)) and, consequently drives the SLR, although the differences become smaller after 2080. Glaciers are expected to add 9.3 cm, but the additional SLR from the overshoot only amounts to 0.75 cm.

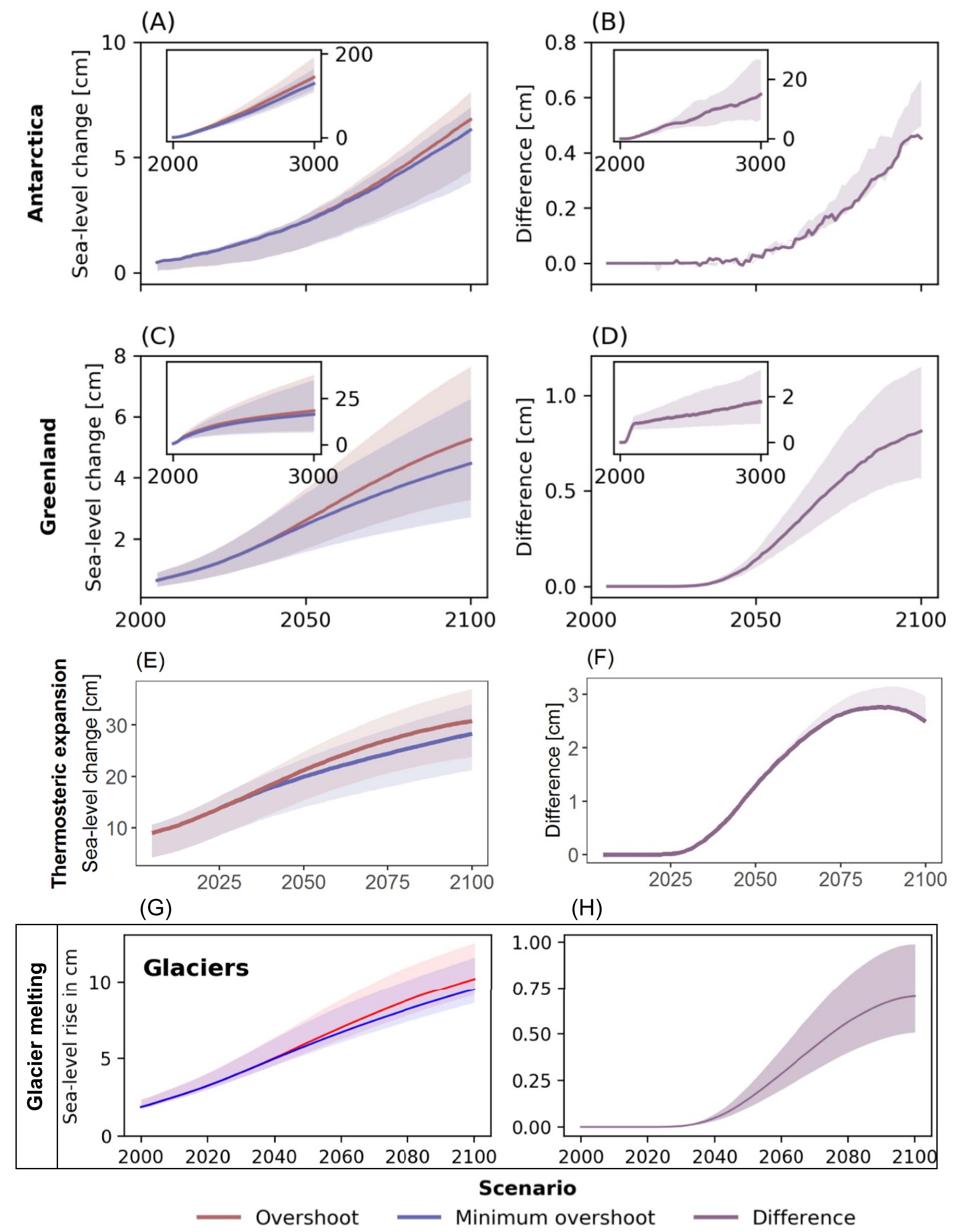

Figure 5. Impact of the overshoot on global sea-level rise. Contribution to sea-level rise by ice-sheet mass loss in Antarctica until 2100 (inlay: until year 3000) (A) as well as effect of full overshoot from pairwise differences compared with minimal overshoot case (B). Absolute and additional contributions to SLR from Greenland ice sheet melting (c) and (d). Absolute and additional contributions to SLR due to thermosteric expansion (e) and (f), and panels (g) and (h) by the SLR emulator of Mengel *et al* (2016). Results for panels (a)–(d) derived with PISM, panels (e) and (f) by UVic, panels (g) and (h) with a semi-empirical model. The shading denotes the uncertainty based on the Greenland melt sensitivity (as explained in detail in the appendix) and the temperature sensitivity of UViC for the case of the Antarctic ice sheet. The shading in (g) and (h) denote the 5th and 95th percentile of the ensemble reflecting the parameter uncertainty in the semi-empirical glacier model. The insets of panels (a)–(d) are derived with the assumption that the geographical distributions of temperature and precipitation anomalies are kept constant at 2100 values.

The Greenland and Antarctic ice-sheets are expected to contribute less to SLR until 2100. Surface melting of the Greenland ice-sheet is driven by air temperatures, which immediately reacts to differences in GMT. The Antarctic ice-sheet is more inert as the melting at the ocean-ice interface depends on increasing water temperatures, which respond with delay to air temperature changes. Antarctica could dominate the contributions to SLR, if the local temperature anomalies in Southern oceans turn out persistent

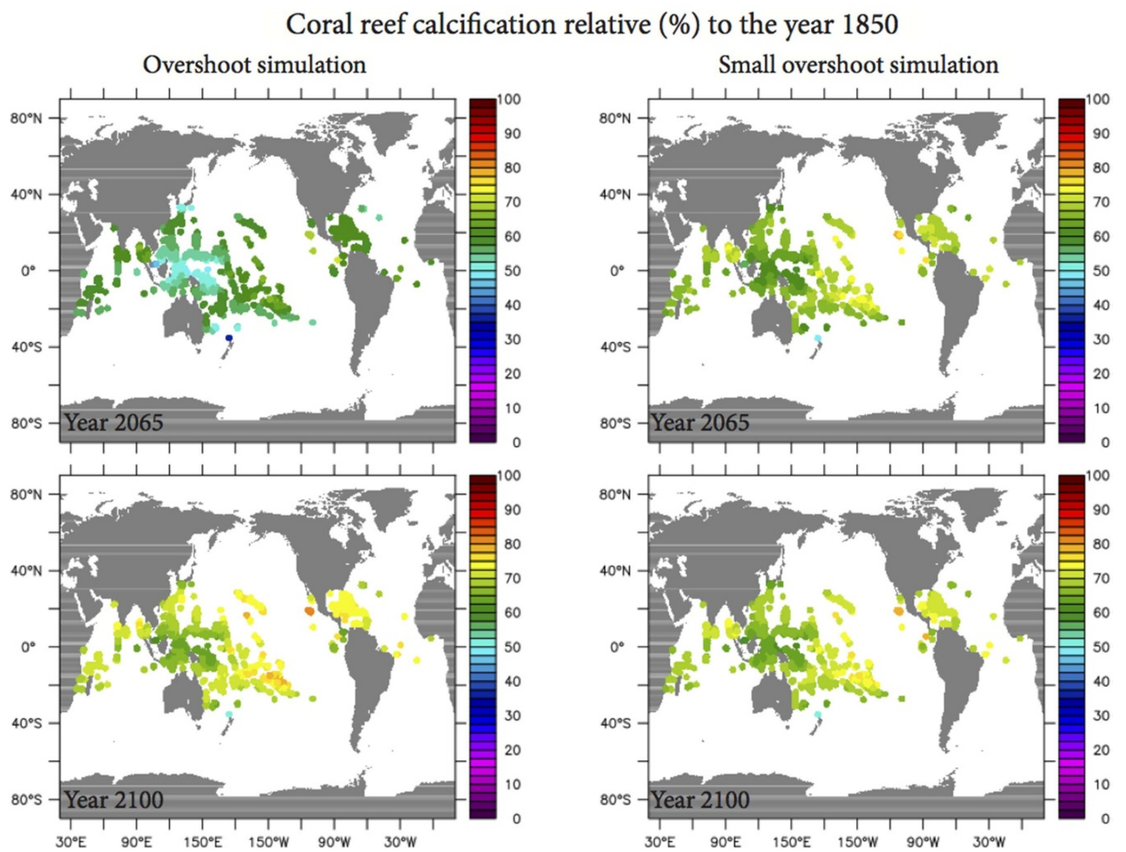

Figure 6. Impact on marine ecosystems measured by the coral calcification rate in % compared to pre-industrial levels. The top row shows results for 2065, whereas the bottom row shows results for 2100.

and therefore increase the melting-rate in Antarctica (figure 5(b) inlay) as small differences can drive long-term changes in ice mass (see Garbe *et al* 2020). Overall the ice-sheets feature more mass loss from melting than mass gains from increasing snow accumulation (Medley and Thomas 2019).

The dynamics of ice-sheets are highly uncertain. In recent analysis the near-term uncertainties regarding the Greenland ice-sheet have been highlighted suggesting a potential underestimation of future ice-sheet looses (Aschwanden *et al* 2021). Also, impacts of SLR are difficult to assess. A recent study attributed nearly 15% of the total economic damage of hurricane Sandy in 2012 on the greater New York area to 9 cm of regional SLR (Strauss *et al* 2021). This highlights that small SLR changes can make a substantial difference. There are no studies that assess the differential impacts of small sea level differences like the one provided here that are in addition to larger future SLR.

3.4. Impact on marine and terrestrial ecosystems

Figure 6 shows the changes of coral calcification rates relative to pre-industrial levels derived with the UVic model. The calcification rates are lowered if water temperatures exceed the optimal level and pH value increases that indicates ocean acidification due to CO_2, which slows the growth and regeneration of coral reefs. The minimal overshoot scenario on the right-hand side shows calcification rates to drop by 40% in 2065 in the area North of Australia. In the full overshoot scenario the calcification rate decreases more severely by 50%. The differences between both scenarios vanish by 2100 as the differences of surface pH values and sea surface temperatures in the relevant areas fade out and thus establish similar environmental conditions allowing calcification rates also to converge (e.g. Albright *et al* 2016). Nonetheless, in both scenarios calcification rates remain substantially below pre-industrial levels (20%–40%).

The calcification rate is calculated using simulated temperature and carbonate chemistry based on the Silverman equation, thereby serving as a proxy for the skeletal growth potential of hard corals. It does not represent the coral stock affected by marine heat waves that become more frequent and other stressors (Frölicher *et al* 2018, Hughes *et al* 2018). Moreover, thermal adaptation is an important, yet uncertain factor for coral reefs' ability to recover (Frieler *et al* 2013, Sully *et al* 2019). Projecting coral stock changes required more specific analysis with ESM (for an earlier analysis, see Frieler *et al* 2013). Finally, coral reef degradation risks irreversible species losses (Trisos *et al* 2020).

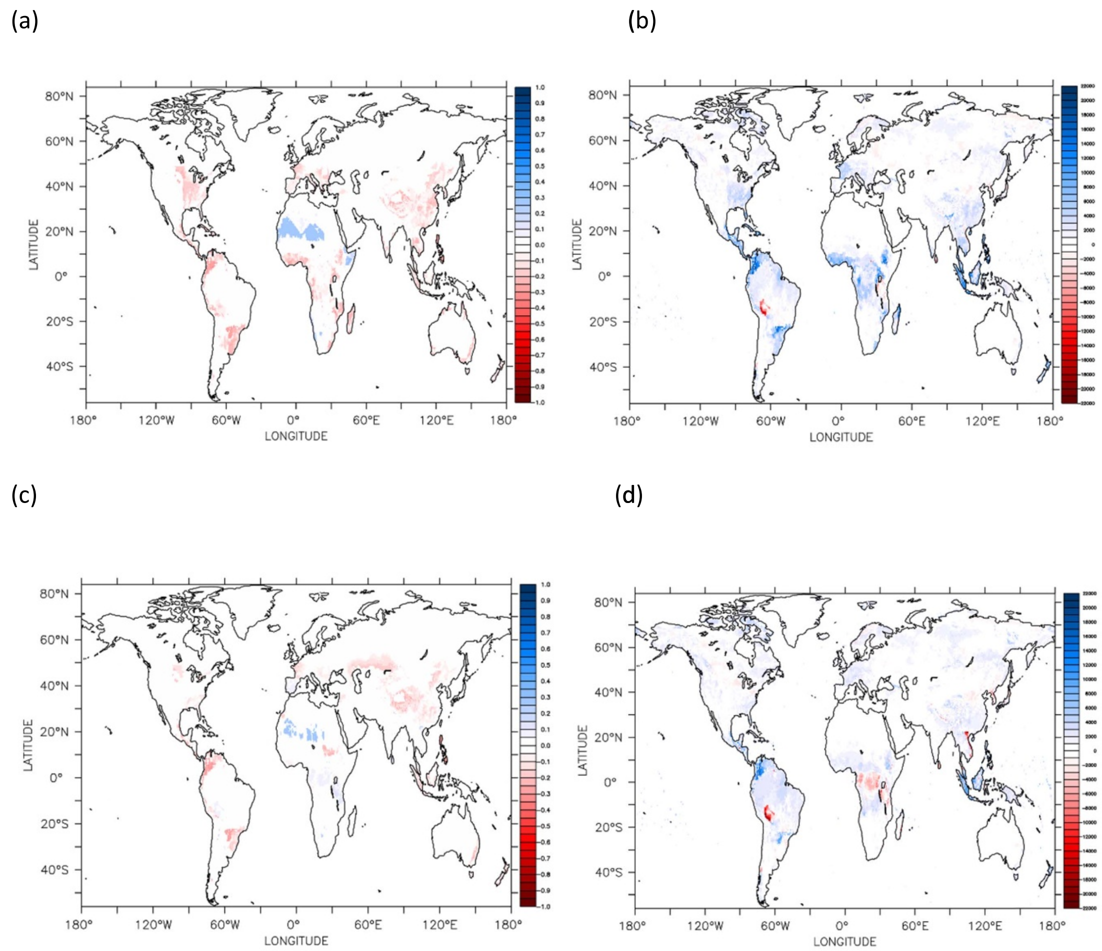

Figure 7. Difference between overshoot and minimal overshoot scenario averaged from 2091–2100 for (a) land-use fraction and (b) total amount of carbon (biomass, litter and soil) in the biosphere (gC m^2). Increasing land-use diminishes carbon stored in biomass in, e.g. central Africa.

Terrestrial vegetation carbon stocks currently absorb 29% of anthropogenic CO_2 emissions (Friedlingstein *et al* 2022). The analysis of the terrestrial ecosystems using LPJmL does not indicate large-scale and abrupt degradation of vegetation carbon pools due to changes in climate conditions of temperature, CO_2-concentration and precipitation derived from UVic. Vegetation carbon pools (figures 7(b) and (d)) are primarily driven by differences in land-use patterns of the two scenarios derived with the REMIND-MAgPIE model (figures 7(a) and (c)). To validate this conclusion, LPJmL has been run with differences in climate variables but frozen land-use patterns 2005–2100, which does not show spatially concentrated differences. The results indicate that the main differences are explained by ubiquitous CO_2 fertilization. In both scenarios carbon losses are projected by 2100 in some regions, incl. North-America, Eurasia, and Northwest of Latin-America (figure S9).

Large-scale and abrupt changes in terrestrial vegetation have been detected in a model ensemble only if global warming exceeds 2.5 °C compared to pre-industrial levels (Drijfhout *et al* 2015). The results suggest that a carbon budget overshoot does not imply additional risks to the integrity of vegetation carbon pools, whereas additional wide-area CO_2 fertilization increases vegetation carbon pools. Differences in land-use change related to afforestation and bioenergy production cause differences in vegetation carbon pools. The role of additional carbon injected into the carbon cycle in the overshoot scenario increases the resilience of terrestrial vegetation systems, while it tends to harm maritime systems due to acidification along with warming oceans.

3.5. Economic impacts and extreme event exposure

The impact of global warming on GDP as well as the differential effect caused by the additional overshoot strongly depends on the permanence parameter. OECD countries, as an aggregate, are expected to slightly benefit due to increasing GDP in both scenarios, whereas non-OECD countries are expected to experience substantial negative consequences for their economies that are even more sever in the scenario with full overshoot. The positive impact on the

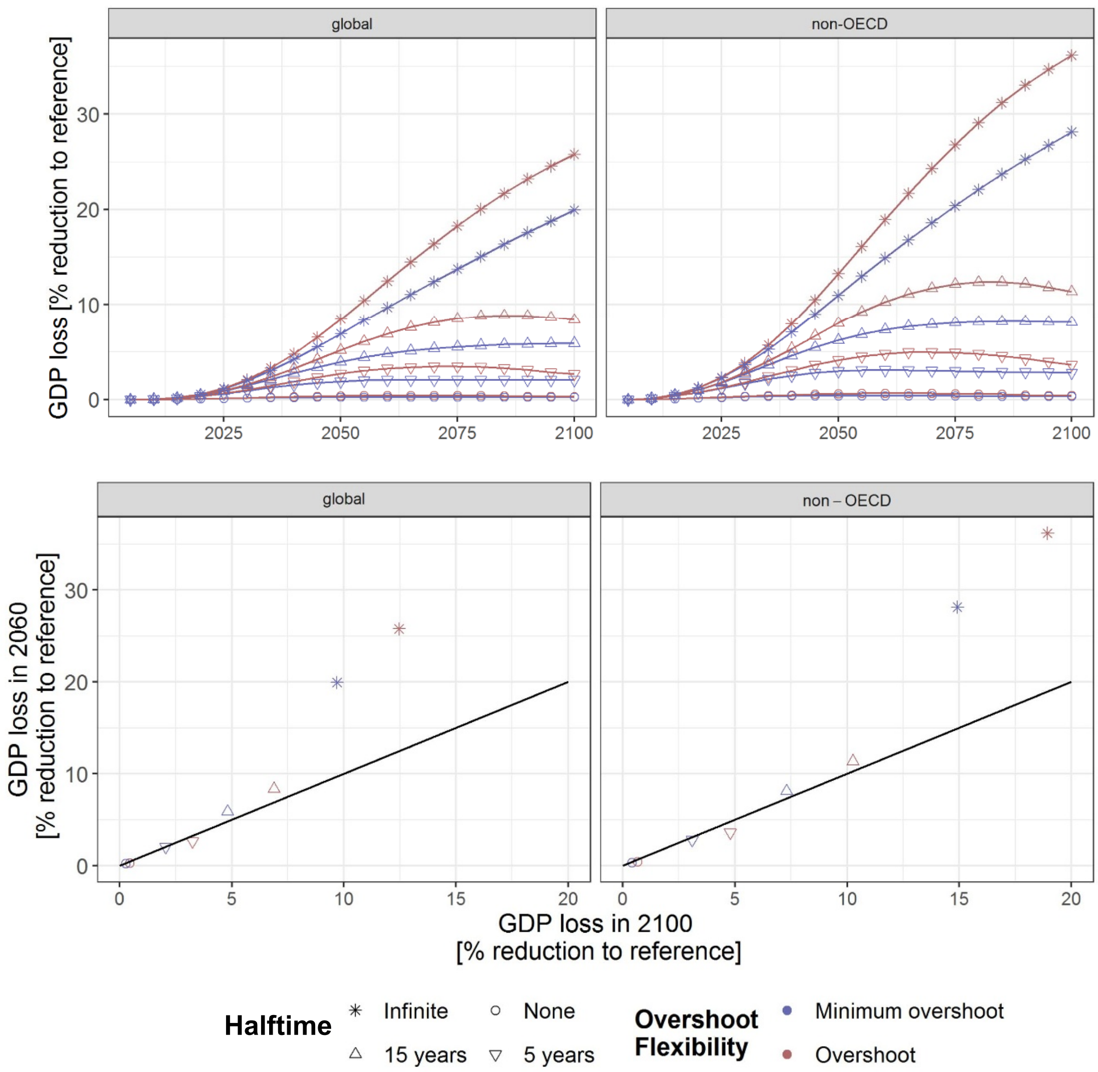

Figure 8. Macroeconomic damages as a percentage of GDP for the world and the aggregate of non-OECD countries differentiated by the overshoot flexibility and the assumption about persistence of damages. 'Infinite' and 'none' represent the extreme values, whereas 5 and 15 year persistence are in the range of modeled and estimated values.

OECD is due to the hump-shaped quadratic function, where many regions in OECD countries at higher latitudes benefit from moderate temperature increases. Non-OECD countries already experience temperatures exceeding the optimal level and, therefore, additional warming as well as a temperature overshoot aggravate the negative effect on GDP (figure 8(b)).

Under the minimal overshoot scenario the relative reduction of global GDP stabilizes (5 year permanence) or keeps on growing slightly (15 year permanence), whereas the difference peaks in the overshoot scenario in the second half of the 21st century and by 2100 a substantial gap still remains that depends on the assumed permanence. In case of 5 year permanence the global GDP reduction in the scenario without overshoot is expected to grow to 2% in 2060 stabilizing afterwards, while it peaks at 3.2% in case with full overshoot and converges slowly towards the no-overshoot case. For a 15 year persistence without overshoot the overall GDP effect more than doubles and the gap continues to grow until 2100 despite temperature differences converging. Again, the effects in non-OECD countries are substantially stronger than the global average. Overall, the permanence parameter is crucial because it suggests to limit global warming to low levels and to avoid the temperature to overshoot.

Assumptions about halftime parameter are highly uncertain. Burke *et al* (2015) implicitly assumed infinite persistence. Econometric estimations found that tropical cyclone events have on average a negative impact on GDP exceeding 15 years (Hsiang and Jina 2014, Krichene *et al* 2021). So far, econometric research has not uncovered the mechanisms that cause the permanent GDP reduction in the years following temperature anomalies. Theoretical and quantitative model research has shown that the alternative approaches of modeling economic

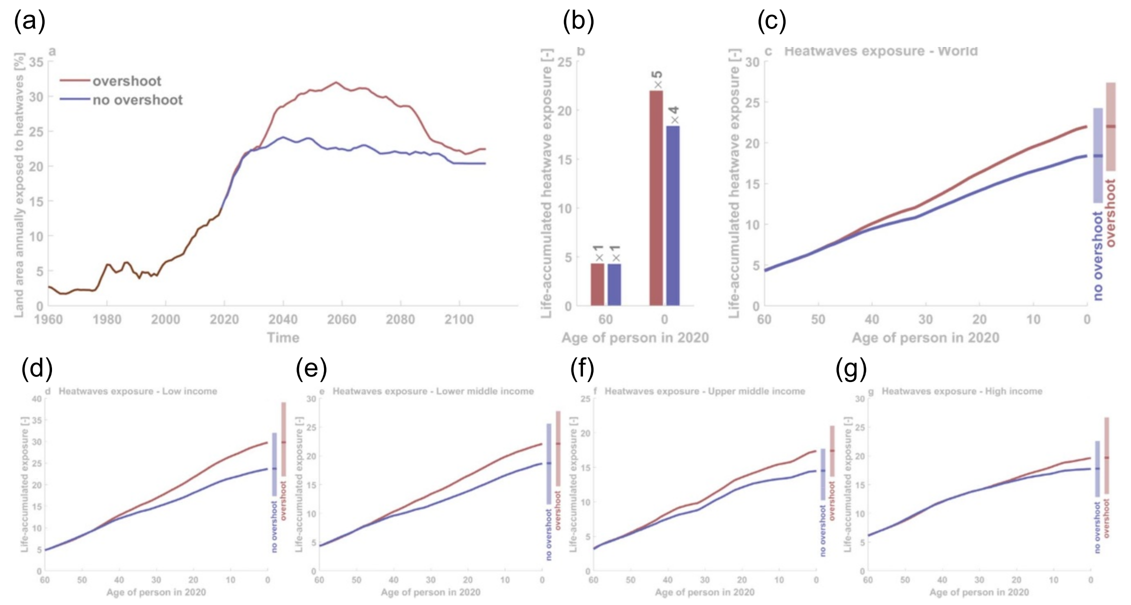

Figure 9. Lifetime exposure to extreme heatwaves under minimal and full overshoot. (a) Total land area annually exposed to extreme heat waves. (b) Lifetime heat wave exposure for different birth cohorts; and associated exposure multiplication factors relative to the 1960 birth cohort. (c) Exposure multiplication factors relative to the 1960 birth cohort for all generations born between 1960 and 2020. (d)–(g) Same as (c) but for different regions depending on per-capita income; note the different scaling on the vertical axes.

damages matters because different macroeconomic transmission channels lead to broadly different transmission channels. An equivalent GDP reduction following a shock results in halftimes between 3 and 40 years (Piontek *et al* 2018). Improved economic estimations are required to better understand the immediate economic impact as well as the longer-lasting macroeconomic adjustment processes. Also, the damage functions do not cover all feedbacks of socioeconomic system with natural systems, such as SLR and extreme events (Rising *et al* 2022) that are treated separately in this study.

Lifetime extreme event exposure is also sensitive to the carbon budget overshoot. Figure 9(a) depicts a substantial increase of total global land area affected by heat waves in the non-overshoot scenario and at maximum it is two thirds higher in the full overshoot scenario. Figure 9(b) shows the cumulative effect on people being born or having reached the age of 60 in 2020, while figure 9(c) depicts the results for all cohorts in between. Under the no-overshoot scenario newborns in 2020 will be exposed five times more to heat waves during their lifetime than people aged 60 years in 2020. This value increase by 25% for newborns as a result of the carbon budget overshoot. The comparison of countries differentiated by income groups in figures 9(d)–(g) shows that the additional heatwave exposure is already higher and increases more strongly in lower-middle income countries than in high-income countries. This pattern is pronounced for newborns and young people. In low-income countries the life expectancy is substantially lower and, therefore, the curve flattens out for people being relatively old today. As highlighted in Thiery *et al* (2021) climate change is the dominant driver, while increasing life-expectancy is only a minor factor. Although temperature increases in tropical regions are smaller due to the polar amplification the increase of heat-wave frequency results from the already high exposure in these regions.

We find similar changes, albeit with less severe differences, for crops failures, droughts, river floods and tropical cyclones. The crops failure indicator shows reduced exposure in the full overshoot case, particularly in high income countries, due to the CO_2 fertilization effect. For wildfire exposure the uncertainty dominates. Higher income countries show a slight increase because they host a high share of boreal forests that are more sensitive than rain forests in tropical countries that typically enjoy lower incomes. Note: the modeling only includes wildfires caused by natural events, e.g. lightning, but not fires caused human activities.

Cumulative extreme event exposure over the lifespan of people provides a perspective on differences in their expected biographies. These differences can have potential knock-on effects on health, property and human capital formation (including schooling). Empirical research identified persistent effects of extreme events on socioeconomic variables in low-income countries (e.g. Groppo and Kraehnert 2017).

4. Discussion and conclusion

The quest for a temporary overshoot of a long-term climate target in the context of the 1.5 °C target needs to consider intertemporal trade-offs and differentiate them regionally. The assessment requires a broad multidisciplinary and comprehensive analysis that maps out various risks and benefits for a set of scenarios. So far, most studies focused on specific issues in separate, disciplinary analysis using scenarios that are not compatible with each other. Such a specialized, yet fragmented approach bears limitations. First, the scenarios are not harmonized and therefore magnitudes of effects are difficult to compare; this includes huge differences (i) the choice of overshooting temperature, CO_2 concentration or cumulative emissions, (ii) the duration and magnitude of the overshoot and (iii) treatment of other climate forcers than only CO_2 as well as land-use change. Second, the systems under investigation and the geographical and temporal boundaries and resolution differ.

In this study we have harmonized the scenarios and included emissions of CO_2, other GHG, other short-lived climate forcers and land-use changes. The resulting overshoot of 700 $GtCO_2$ or 0.35 °C is at the upper end of the scenarios assessed by the WG3 of the IPCC, but still smaller than many studies used for assessing additional climate risks. Our analysis is summarized in table 1, with four major findings.

First, global climate variables show no or only small differences at the end of the 21st century; For instance, by 2100, 80% of the peak GMT difference is closed. However, differentiation of the climate system identifies path-dependencies, e.g. the polar amplification remains more persistent than GMT anomalies. Also, CO_2-concentrations in both scenarios are similar in 2100, but additional loss of soil carbon from permafrost thawing is off-set by stronger CO_2 fertilization of the vegetation carbon stock and more ocean carbon up-take. The global temperature overshoot triggers a variety of mostly regional effects, such as sea ice losses, slowing of the meridional overturning and lower coral calcification rates. Global SLR is a notable special case. Antarctic ice sheet melting can overtake thermosteric expansion as the major driver after 2100. This is subject to uncertainties about the strength and persistence of polar amplification of global warming and the response of the southern oceans. Thus, a carbon budget overshoot scenario of the magnitude and duration we explored in this study will lead to only small residual relative differences of global climate variables in 2100, like GMT, but there can be more notable and persistent differences in key climatic and environmental sub-systems that vary regionally.

Second, many impacts strongly depend on the global temperature trajectory causing path-dependent processes in socioeconomic systems, particularly in tropical regions with high base year temperatures. Regarding extreme weather event the overshoot can increase life time exposure for young generations substantially with various knock-on effects such as potential reductions of human capital formation. Furthermore, negative impacts on GDP can cumulate and lead to persistent differences. Also here, countries with the disadvantage of high base year temperature are more affected, despite the comparatively smaller temperature increase. Spatial heterogeneity is crucial because countries in the most sensitive regions are developing and emerging economies, typically non-OECD countries, with comparatively lower per-capita incomes.

Third, on the mitigation side non-OECD countries also respond more sensitively to variations of the overshoot. Until 2100 both scenarios lead to similar amounts of cumulative carbon removals but to remarkable differences in land-use, with more afforestation in case with no-overshoot but less removals relying on BECCS. Furthermore, limiting the overshoot requires stronger near-term emission reductions and removals, which causes substantially higher near-term GDP losses with much larger differences in non-OECD countries. The differences turn into a slight benefit of limiting the overshoot after 2050. Thus, the trade-offs between short term mitigation costs and longer-term impacts and damages are stronger in developing and emerging economies than in OECD countries.

Fourth, additional CO_2 emissions in the overshoot scenario act very differently in terrestrial and marine systems. While the terrestrial vegetation is fertilized, marine ecosystems like coral reefs are subject to diminishing natural resilience due to ocean acidification that adds to the additional pressure of increasing sea surface temperatures. When the impacts of the overshoot propagate into the deeper ocean, they will persist for centuries to millenia (Mathesius *et al* 2015), even after the scenarios converge for GMT and CO_2. For the scenarios studied here the major differences in terrestrial vegetation are triggered by human activities like afforestation and reduced deforestation, while marine environments can be strongly affected by the changes in temperatures and CO_2-concentrations.

Future overshoot assessments can benefit from deepening model integration in four areas. First, the mitigation and removal scenarios require improved framing to fully represent the diversity and heterogeneity of socioeconomic systems. The requirement for equitable mitigation burden sharing can lead to very different global scale and regional allocation of CDR (Bauer *et al* 2020a). Second, inclusion of additional direct human forcers with spatial resolution help to assess systems under multiple pressures, including nitrogen use, overfishing, water and air pollution, and dam building. Potentially large-scale changes in land use deserve additional analysis, including local climate feedbacks, e.g. UVic results indicate that land-use patterns cause differences in precipitation due to

Table 1. Summary of results regarding temporal and geographical differences between scenarios. Vegetation carbon pools include all terrestrial vegetation.

System	Component	Indicator	Minimum overshoot	Full overshoot	Persistency in 2100	Regional heterogeneity	Comment
Mitigation	Overshoot	Max. cumulative emissions above carbon budget	50 $GtCO_2$	700 $GtCO_2$	None, by assumption		Peak in 2060
	CDR deployment	Cumulative carbon removal 2020–2100	800 $GtCO_2$	950 $GtCO_2$	Storage is assumed permanent; persistent land-use changes	With low overshoot more afforestation in tropical countries	Substantial shift from afforestation to BECCS and DACS
	Climate policy	Carbon price in 2030	50 USD/tCO_2	540 USD/tCO_2	Relative difference constant by assumption	Uniform	Shape strongly non-linear
	Mitigation costs	Reduction in GDP from baseline	1.2%	3.5%	Near- and mid-term losses major effect; reversal after 2050	With low overshoot OECD countries 1.2%, but non-OECD countries 5.9%	Immediate effect on non-OECD GDP 12% in 2030
Climate system	Carbon cycle	Peak CO_2-concentration	424 ppmv in 2030	474 ppmv in 2050	With full overshoot CO_2 concentration is slightly lower	Uniformly mixed in global atmosphere	
		Change of $GtCO_2$ in pools 2020–2100	Vegetation +174, permafrost −58 soil −183, ocean +336, sum = + 269	Vegetation +112, permafrost −80, soil −136, ocean +407, total +303	Vegetation reversible, permafrost persistent, Ocean slowly reversible	Persistent changes on terrestrial carbon pools that net out roughly net out	CO_2 fertilization effect is pervasive
	Global mean temperature	GMT in 2065	1.4 °C (−0.2; +0.4)	1.8 °C (−0.2; +0.4)	20% of peak difference	Polar amplification in 2100 is disproportional, particularly in the arctic sea	Fast thermal response to CO_2 emissions and removals
	Ocean heat content	Anomaly in 2080	$0.67^{*}10^{24}$ Joule	$0.88^{*}10^{24}$ Joule	>90% of peak difference	Polar amplification and slow movement to deeper layers	Slow thermal reaction; various knock-on effects in ocean
	Sea ice	Arctic sea ice area	0.4 million km2 drop from 2020	0.61 Million km^2 further reduction	40% of peak difference remaining	Arctic effect stronger than Antarctic	Sea ice is crucial component for ocean currents
	Meridional overturning	Reduction compared to 2020	1 Sv in 2100	0.88 Sv in 2100 further reduction	Fully persistent, convergence by 2100	Atlantic ocean, northern hemisphere	
	Sea level rise	Increase compared to 2020	39.7 cm in 2100	Additional 3.6 cm in 2100	No convergence between scenarios before 2100	SLR global, but ice and glacier melting affects high altitude and polar regions	Also long after 2100 SLR continues under low overshoot

(Continued.)

Table 1. (Continued.)

Eco-system	Maritime ecosystems, coral reefs	Drop of calcification rate in 2065 below 1850 levels	Up to 40%	Up to 50%	Near full reversibility; coral stocks might show different behavior	Tropical regions, mostly South East Asia, Australia	CO_2 has adverse effects
	Vegetation	Carbon density	Concentrated changes due to land-use change (e.g. afforestation)	No additional climate induced losses from overshoot	More forest carbon stocks in low-overshoot scenario	Largest changes in tropical regions with high afforestation rates	LUC dominates climate; CO_2 fertilize enhances resilience,
Impacts and Damages	Lifetime exposure to climate extremes	Projected lifetime exposure by age cohorts in 2020	Substantial increase of cumulative extreme weather event exposure, particularly heat waves	Significantly stronger heat wave exposure	Cumulative effects can affect socioeconomic developments (human capital) in the long-run	Hot countries (usually non-OECD) are affected more severely	Heat waves most sensitive, other impact sector show different regional results
	GDP reductions	% GDP reduction from baseline	5 yr perm.: 2.1% in 2070 15 yr perm.: 5.9% in 2100	5 yr perm.: 3.4% in 2070 15 yr perm.: 8.3% in 2100	5 yr perm.: 45% of peak difference 15 yr perm.: no convergence	Non-OECD with 5 yr perm 3.1 vs 4.8% in 2060 and 0.8% difference in 2100.	Huge uncertainty about the permanence parameter

evapotranspiration differences. Furthermore, EMICs can provide useful insights on process interactions in the global terrestrial and marine carbon cycle that allow to study net effects of overshoot scenarios on biogeochemical cycles interacting with climate (e.g. Drüke *et al* 2021). Third, overshoot magnitude and duration need to be consistent between IAM scenarios and subsequent ESM evaluation. Fourth, the large and near-term land-use related CDR deployment, particularly in the low-overshoot scenario, requires more in-depth investigation, including biodiversity and socioeconomic consequences.

Models can derive an increasing amount of information. Integrative analysis frameworks are needed to enhance the quantification of trade-offs and uncertainties. Our analysis shows that it is not only important to consider global systems' dynamics and lock-ins, but also to represent regional and spatial dimensions to improve the understanding of the various distributional issues and trade-offs. Our analysis suggests that the quest of overshooting the carbon budget implies strong trade-offs between mitigation costs and impacts for developing and emerging economies. Assessments with a broad coverage of various systems need to link an increasing number of complex models, which raises methodological challenges on interfaces and uncertainties as well as the interpretation of results. Quantifying uncertainties within models as well as improved methods for the propagation of uncertainties through a chain of interacting models would help to enhance the integrated trade-off assessment of overshoots. To honor the complexity, diversity and uncertainty of the trade-off relationship future analysis needs to be embedded into a broader assessment framework that includes aggregate welfare metrics as well as multi-indicator frameworks, e.g. the sustainable development indicators as a basis.

Data availability statement

The data that support the findings of this study are openly available at the following URL/DOI: 10.5281/zenodo.7777223. Data will be available from 28 April 2023.

Code and data availability

The code and data is available at https://zenodo.org/deposit/7777223. The code for the model REMIND 2.7 is available at https://gitlab.pik-potsdam.de/REMIND/REMIND/ (revision r8644) and for the MAgPIE 4.1 model at https://github.com/magpiemodel/magpie (ID: 950bc7a08fd0e6c8f790c1399c7837133233e2fc).

The PISM code used for the Antarctic Ice Sheet simulations presented in this study is openly available and can be obtained from Zenodo under https://doi.org/10.5281/zenodo.7777927

Acknowledgments

Development of PISM is supported by NSF Grant Nos. PLR-1603799 and PLR-1644277 and NASA Grant No. NNX17AG65G J Garbe, R Winkelmann and M Zeitz were supported by the Leibniz Association (project 'DominoES') as well as by the Deutsche Forschungsgemeinschaft (DFG) through Grant No. WI4556/3-1. D P Keller, Dr Jessica Strefler and N Bauer received funding from the German Research Foundation's Priority Program SPP 1689 'Climate Engineering' (CDR-MIA project KE 2149/2-1). This work was supported by the European Union's Horizon 2020 research and innovation programme under Grant Agreement No. 821124 (NAVIGATE). The authors gratefully acknowledge the European Regional Development Fund (ERDF), the German Federal Ministry of Education and Research and the Land Brandenburg for supporting this project by providing resources on the high-performance computer system at the Potsdam Institute for Climate Impact Research.

ORCID iDs

Nico Bauer https://orcid.org/0000-0002-0211-4162
David P Keller https://orcid.org/0000-0001-6780-3869
Julius Garbe https://orcid.org/0000-0003-3140-3307
Kristine Karstens https://orcid.org/0000-0002-5860-9789
Werner von Bloh https://orcid.org/0000-0002-7399-2704
Wim Thiery https://orcid.org/0000-0002-5183-6145
Maria Zeitz https://orcid.org/0000-0001-8129-1329
Matthias Mengel https://orcid.org/0000-0001-6724-9685
Jessica Strefler https://orcid.org/0000-0002-5279-4629
Kirsten Thonicke https://orcid.org/0000-0001-5283-4937
Ricarda Winkelmann https://orcid.org/0000-0003-1248-3217

References

Albright R *et al* 2016 Reversal of ocean acidification enhances net coral reef calcification *Nature* **531** 362–5

Aschwanden A, Bartholomaus T C, Brinkerhoff D J and Truffer M 2021 Brief communication: a roadmap towards credible projections of ice sheet contribution to sea level *Cryosphere* **15** 5705–15

Bauer N *et al* 2018 Global energy sector emission reductions and bioenergy use: overview of the bioenergy demand phase of the EMF-33 model comparison *Clim. Change* **163** 1553–68

Bauer N, Bertram C, Schultes A, Klein D, Luderer G, Kriegler E, Popp A and Edenhofer O 2020a Quantification of an

efficiency—sovereignty trade-off in climate policy *Nature* **588** 261–6
Bauer N, Klein D, Humpenöder F, Kriegler E, Luderer G, Popp A and Strefler J 2020b Bio-energy and CO_2 emission reductions: an integrated land-use and energy sector perspective *Clim. Change* **163** 1675–93
Boucher O, Halloran P R, Burke E J, Doutriaux-Boucher M, Jones C D, Lowe J, Ringer M A, Robertson E and Wu P 2012 Reversibility in an Earth system model in response to CO_2 concentration changes *Environ. Res. Lett.* **7** 024013
Bueler E and Brown J 2009 Shallow shelf approximation as a "sliding law" in a thermomechanically coupled ice sheet model *J. Geophys. Res.* **114** F03008
Burke M, Hsiang S M and Miguel E 2015 Global non-linear effect of temperature on economic production *Nature* **527** 235–9
Calov R and Greve R 2005 A semi-analytical solution for the positive degree-day model with stochastic temperature variations *J. Glaciol.* **51** 173–5
Dellink R, Chateau J, Lanzi E and Magné B 2017 Long-term economic growth projections in the shared socioeconomic pathways *Glob. Environ. Change* **42** 200–14
Drijfhout S, Bathiany S, Beaulieu C, Brovkin V, Claussen M, Huntingford C, Scheffer M, Sgubin G and Swingedouw D 2015 Catalogue of abrupt shifts in intergovernmental panel on climate change climate models *Proc. Natl Acad. Sci. USA* **112** E5777–86
Drouet L *et al* 2021 Net zero-emission pathways reduce the physical and economic risks of climate change *Nat. Clim. Change* **11** 1070–6
Drüke M, von Bloh W, Petri S, Sakschewski B, Schaphoff S, Forkel M, Huiskamp W, Feulner G and Thonicke K 2021 CM2Mc-LPJmL v1.0: biophysical coupling of a process-based dynamic vegetation model with managed land to a general circulation model *Geosci. Model Dev.* **14** 4117–41
Friedlingstein P *et al* 2022 Global carbon budget 2022 *Earth Syst. Sci. Data* **14** 4811–900
Friedlingstein P, Meinshausen M, Arora V K, Jones C D, Anav A, Liddicoat S K and Knutti R 2014 Uncertainties in CMIP5 climate projections due to carbon cycle feedbacks *J. Clim.* **27** 511–26
Frieler K, Meinshausen M, Golly A, Mengel M, Lebek K, Donner S D and Hoegh-Guldberg O 2013 Limiting global warming to 2 °C is unlikely to save most coral reefs *Nat. Clim. Change* **3** 165–70
Frölicher T L, Fischer E M and Gruber N 2018 Marine heatwaves under global warming *Nature* **560** 360–4
Garbe J, Albrecht T, Levermann A, Donges J F and Winkelmann R 2020 The hysteresis of the Antarctic Ice Sheet *Nature* **585** 538–44
Gleckler P J, Wigley T M L, Santer B D, Gregory J M, AchutaRao K and Taylor K E 2006 Krakatoa's signature persists in the ocean *Nature* **439** 675
Gregory J M *et al* 2013 Climate models without preindustrial volcanic forcing underestimate historical ocean thermal expansion *Geophys. Res. Lett.* **40** 1600–4
Groppo V and Kraehnert K 2017 The impact of extreme weather events on education *J. Popul. Econ.* **30** 433–72
Heck V, Gerten D, Lucht W and Popp A 2018 Biomass-based negative emissions difficult to reconcile with planetary boundaries *Nat. Clim. Change* **8** 151–5
Hewitt A J, Booth B B B, Jones C D, Robertson E S, Wiltshire A J, Sansom P G, Stephenson D B and Yip S 2016 Sources of uncertainty in future projections of the carbon cycle *J. Clim.* **29** 7203–13
Hoffman F M *et al* 2014 Causes and implications of persistent atmospheric carbon dioxide biases in earth system models *J. Geophys. Res. Biogeosci.* **119** 141–62
Hofmann M, Mathesius S, Kriegler E, Vuuren D P and Van, Schellnhuber H J 2019 Strong time dependence of ocean acidification mitigation by atmospheric carbon dioxide removal *Nat. Commun.* **10** 5592
Hsiang S M and Jina A S 2014 The causal effect of environmental catastrophe on long-run economic growth: evidence from 6700 cyclones *Working Paper No. 20352* (National Bureau of Economic Research) (https://doi.org/10.3386/w20352)
Hughes T P *et al* 2018 Spatial and temporal patterns of mass bleaching of corals in the Anthropocene *Science* **359** 80–83
Johansson D J A, Azar C, Lehtveer M and Peters G P 2020 The role of negative carbon emissions in reaching the Paris climate targets: the impact of target formulation in integrated assessment models *Environ. Res. Lett.* **15** 124024
Jones C D *et al* 2016 Simulating the Earth system response to negative emissions *Environ. Res. Lett.* **11** 095012
KC S and Lutz W 2017 The human core of the shared socioeconomic pathways: population scenarios by age, sex and level of education for all countries to 2100 *Glob. Environ. Change* **42** 181–92
Krichene H, Geiger T, Frieler K, Willner S N, Sauer I and Otto C 2021 Long-term impacts of tropical cyclones and fluvial floods on economic growth—empirical evidence on transmission channels at different levels of development *World Dev.* **144** 105475
Kriegler E *et al* 2014 The role of technology for achieving climate policy objectives: overview of the EMF 27 study on global technology and climate policy strategies *Clim. Change* **123** 353–67
Kriegler E *et al* 2017 Fossil-fueled development (SSP5): an energy and resource intensive scenario for the 21st century *Glob. Environ. Change* **42** 297–315
Lange S *et al* 2020 Projecting exposure to extreme climate impact events across six event categories and three spatial scales *Earths Future* **8** e2020EF001616
MacDougall A H 2013 Reversing climate warming by artificial atmospheric carbon-dioxide removal: can a holocene-like climate be restored?: RETURN TO THE HOLOCENE *Geophys. Res. Lett.* **40** 5480–5
Mathesius S, Hofmann M, Caldeira K and Schellnhuber H J 2015 Long-term response of oceans to CO_2 removal from the atmosphere *Nat. Clim. Change* **5** 1107–13
Matthews H D, Gillett N P, Stott P A and Zickfeld K 2009 The proportionality of global warming to cumulative carbon emissions *Nature* **459** 829–32
McGuire A D *et al* 2018 Dependence of the evolution of carbon dynamics in the northern permafrost region on the trajectory of climate change *Proc. Natl Acad. Sci.* **115** 3882–7
Medley B and Thomas E R 2019 Increased snowfall over the Antarctic Ice Sheet mitigated twentieth-century sea-level rise *Nat. Clim. Change* **9** 34–39
Meinshausen M, Meinshausen N, Hare W, Raper S C B, Frieler K, Knutti R, Frame D J and Allen M R 2009 Greenhouse-gas emission targets for limiting global warming to 2 °C *Nature* **458** 1158–62
Melnikova I, Boucher O, Cadule P, Ciais P, Gasser T, Quilcaille Y, Shiogama H, Tachiiri K, Yokohata T and Tanaka K 2021 Carbon cycle response to temperature overshoot beyond 2 °C: an analysis of CMIP6 models *Earths Future* **9** e2020EF001967
Mengel M, Levermann A, Frieler K, Robinson A, Marzeion B and Winkelmann R 2016 Future sea level rise constrained by observations and long-term commitment *Proc. Natl Acad. Sci. USA* **113** 2597–602
Mengis N *et al* 2020 Evaluation of the University of Victoria earth system climate model version 2.10 (UVic ESCM 2.10) *Geosci. Model Dev.* **13** 4183–204
Newell R G, Prest B C and Sexton S E 2021 The GDP-Temperature relationship: implications for climate change damages *J. Environ. Econ. Manage.* **108** 102445
Palter J B, Frölicher T L, Paynter D and John J G, 2017 Climate, ocean circulation, and sea level changes under stabilization and overshoot pathways to 1.5 K warming. *Earth Syst. change Clim. Scenarios* **9** 817–28
Pihl E *et al* 2021 Ten new insights in climate science 2020—a horizon scan *Glob. Sustain.* **4** e5

Piontek F, Kalkuhl M, Kriegler E, Schultes A, Leimbach M, Edenhofer O and Bauer N 2018 Economic growth effects of alternative climate change impact channels in economic modeling *Environ. Resource Econ.* **73** 1357–85

Rao S *et al* 2017 Future air pollution in the shared socio-economic pathways *Glob. Environ. Change* **42** 346–58

Realmonte G, Drouet L, Gambhir A, Glynn J, Hawkes A, Köberle A C and Tavoni M 2019 An inter-model assessment of the role of direct air capture in deep mitigation pathways *Nat. Commun.* **10** 3277

Reese R, Albrecht T, Mengel M, Asay-Davis X and Winkelmann R 2018 Antarctic sub-shelf melt rates via PICO *Cryosphere* **12** 1969–85

Riahi K *et al* 2021 Cost and attainability of meeting stringent climate targets without overshoot *Nat. Clim. Change* **11** 1063–9

Rising J, Tedesco M, Piontek F and Stainforth D A 2022 The missing risks of climate change *Nature* **610** 643–51

Rogelj J *et al* 2018 Mitigation pathways compatible with 1.5 °C in the context of sustainable development *Global Warming of 1.5 °C an IPCC Special Report on the Impacts of Global Warming of 1.5 °C above Pre-Industrial Levels and Related Global Greenhouse Gas Emission Pathways, in the Context of Strengthening the Global Response to the Threat of Climate Change* (Intergovernmental Panel on Climate Change) ch 2

Rogelj J, Forster P M, Kriegler E, Smith C J and Séférian R 2019 Estimating and tracking the remaining carbon budget for stringent climate targets *Nature* **571** 335–42

Schaphoff S *et al* 2018 LPJmL4—a dynamic global vegetation model with managed land—Part 1: model description *Geosci. Model Dev.* **11** 1343–75

Schultes A, Piontek F, Soergel B, Rogelj J, Baumstark L, Kriegler E, Edenhofer O and Luderer G 2021 Economic damages from on-going climate change imply deeper near-term emission cuts *Environ. Res. Lett.* **16** 104053

Smith P *et al* 2015 Biophysical and economic limits to negative CO_2 emissions *Nat. Clim. Change* **6** 42–50

Strauss B H, Orton P M, Bittermann K, Buchanan M K, Gilford D M, Kopp R E, Kulp S, Massey C, Moel H and De, Vinogradov S 2021 Economic damages from Hurricane Sandy attributable to sea level rise caused by anthropogenic climate change *Nat. Commun.* **12** 2720

Strefler J, Bauer N, Humpenöder F, Klein D, Popp A and Kriegler E 2021b Carbon dioxide removal technologies are not born equal *Environ. Res. Lett.* **16** 074021

Strefler J, Kriegler E, Bauer N, Luderer G, Pietzcker R C, Giannousakis A and Edenhofer O 2021a Alternative carbon price trajectories can avoid excessive carbon removal *Nat. Commun.* **12** 2264

Sully S, Burkepile D E, Donovan M K, Hodgson G and van Woesik R 2019 A global analysis of coral bleaching over the past two decades *Nat. Commun.* **10** 1264

Thiery W *et al* 2021 Intergenerational inequities in exposure to climate extremes *Science* **374** 158–60

Tokarska K B and Zickfeld K 2015 The effectiveness of net negative carbon dioxide emissions in reversing anthropogenic climate change *Environ. Res. Lett.* **10** 094013

Trisos C H, Merow C and Pigot A L 2020 The projected timing of abrupt ecological disruption from climate change *Nature* **580** 496–501

Winkelmann R, Martin M A, Haseloff M, Albrecht T, Bueler E, Khroulev C and Levermann A 2011 The potsdam parallel ice sheet model (PISM-PIK)—part 1: model description *Cryosphere* **5** 715–26

Zeitz M, Reese R, Beckmann J, Krebs-Kanzow U and Winkelmann R 2021 Impact of the melt–albedo feedback on the future evolution of the Greenland Ice sheet with PISM-dEBM-simple *Cryosphere* **15** 5739–64

Zickfeld K, Azevedo D, Mathesius S and Matthews H D 2021 Asymmetry in the climate–carbon cycle response to positive and negative CO_2 emissions *Nat. Clim. Change* **11** 613–7

Zickfeld K, MacDougall A H and Matthews H D 2016 On the proportionality between global temperature change and cumulative CO_2 emissions during periods of net negative CO_2 emissions *Environ. Res. Lett.* **11** 055006